

# Optimization of the nanofibrous structure of non-woven mats of electrospun biodegradable nanocomposites using Response Surface Methodology

A. Tsimliaraki<sup>1,2</sup>, S. Svinterikos<sup>1</sup>, S. I. Marras<sup>2</sup>, I. Zuburtikudis<sup>2\*</sup> and C. Panayiotou<sup>1</sup>

<sup>1</sup>*Department of Chemical Engineering, Aristotle University of Thessaloniki, Thessaloniki, Greece*

<sup>2</sup>*Department of Industrial Design Engineering, TEI of Western Macedonia, Kozani, Greece*

## Abstract

Electrospun mats of polymer-clay nanocomposites were prepared in order to study the influence of material and process parameter settings on their morphology. The polymer solution concentration, the flow rate of the injected solution and the organically-modified-clay content of the polymer matrix were the factors chosen to be investigated according to a design of experiments (DoE) within the context of response surface methodology (RSM). The developed quadratic models and the individual and coupling effect of the three factors examined are given. The results suggest that the dominant parameter affecting mats' morphology is polymer solution concentration and that a broader range in the factor settings, especially for concentration, should be used in a subsequent optimization.

## Introduction

Presently, nanofiber manufacturing is one of the key advancements in nanotechnology. For this reason, electrospinning has been widely used as an alternative technique in fabrication of mats consisting of fiber diameters ranging from few nanometers to few micrometers. This is a markedly simple and cost effective process which operates on the principle that the solution is extracted under a high electric field. The final fibrous structure can be tailored by altering the material and process parameters involved, such as the concentration of the polymer solution, the applied voltage, the flow rate, the diameter and angle of the spinneret, the spinning distance, the solution's viscosity and conductivity, just to mention a few [1]. Furthermore, the combination of their nanometric dimensionality, high surface area, porosity, flexibility and mechanical integrity makes the electrospun fibers suitable for several value-added applications, such as tissue engineering, wound dressing, clothing protection, nanoscale and biological adsorption, filter and membrane technology.

During the last decade various polymers, most of which dissolved in solvents, but also some in melt form, have been successfully electrospun into ultra fine fibers [2]. However, there are few studies regarding the electrospinning of polymer/layered silicate

---

\* Corresponding author:

nanocomposites [3-9] and particularly of biodegradable-polymer based nanocomposites, in spite of the fact that they are environmentally friendly with potential applications both as filters and as reinforcing components in other composite systems [2].

In the present work, a novel polymer – clay nanocomposite system is studied. A biodegradable aliphatic polyester was used as a polymer matrix, where organically modified montmorillonite is incorporated. Membranes comprised of various structures of the nanocomposite material were subsequently prepared via electrospinning according to a design of experiments (DoE). An investigation was conducted to identify and quantify the important electrospinning material and processing parameters that affect the morphology of the collected mats and to recognize the experimental settings domain useful for a subsequent optimization.

## **Experimental**

### ***Materials and methods***

The biodegradable aliphatic polyester PBSA by the commercial name 'Bionolle 3001' was supplied by Showa Highpolymer Co., Ltd (Tokyo, Japan). Bionolle 3001 is a copolyester of succinic acid (S), adipic acid (A) and 1,4 butanediol (B) with a composition ratio 40/10/50, respectively. The nanofiller used, was organically modified montmorillonite (Cloisite 25A) and was purchased from Southern Clay Products (Texas, USA), while dichloromethane ( $\text{CH}_2\text{Cl}_2$ ) was obtained from Sigma-Aldrich.

Initially, the nanocomposite materials were prepared in bulk as films according to the same solution casting routine followed in our previous studies [10,11]. The films obtained were dried in vacuum at 40 °C for 24 h. The organoclay content of the produced films was ranging from 0 to 9 wt%. The electrospinning set up used for nanofibres manufacturing was homemade. Dichloromethane was used as a solvent for the preparation of the solutions from the nanocomposite stock materials previously prepared.

The membrane structures were explored by Scanning Electron Microscopy (SEM) using a JEOL microscope, (mod. JSM-840A) and processed by the appropriate software. The generation of the D-optimal design and the subsequent regression analysis was attained with the help of MODDE™ 8.0 software.

### ***Experimental design and responses***

The DoE used included 25 experimental runs, four of which were pure replicates (the experimental space investigated is shown in Fig.1). Three variables were chosen as controllable factors; flow rate (qualitative factor), solution concentration and clay loading in polymer nanocomposite (quantitative factors).

Three responses were defined in order to achieve a more reliable representation of the experimental outcomes. A full picture of each sample's morphology is pursued by the ratio of the average bead and fiber diameters,  $D_{\text{bead}}/D_{\text{fibre}}$ , and the number surface density of beads,  $N_{\text{bead}}$ , as well as the average fiber diameter,  $D_{\text{fibre}}$ .

## **Results and discussion**

### ***Morphology***

SEM photographs of the electrospun mats resulted in five different morphologies depicted at Fig.1: Fibers and a small amount of spindle-like beads (Exp.No4), fibers with a

large amount of spindle-like beads (Exp.No16), pearls-on-string morphology (Exp.No25), only beads (Exp.No9) and, finally, there were two experiments (Exp.No13&18) for which the solution was cast from the spinneret on the collector without previous solvent evaporation. This was observed at low solution concentrations and clay loadings and at very high flow rates. Therefore, it was impossible to take a measurement for any of the three responses at these experimental runs. That reduced the 25 runs to 23.

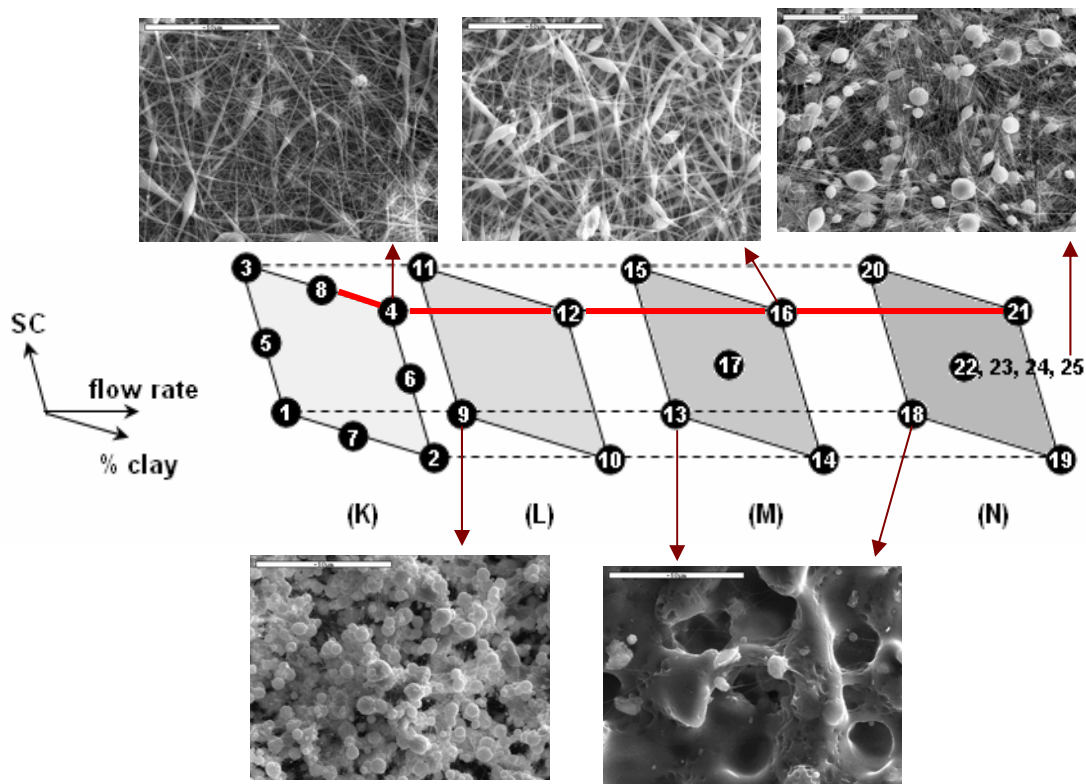


**Fig. 1.** The five indicative morphologies observed overall by SEM at various combinations of factor settings; scale bar at 50  $\mu\text{m}$ . The numbers correspond to the 25 experiments conducted.

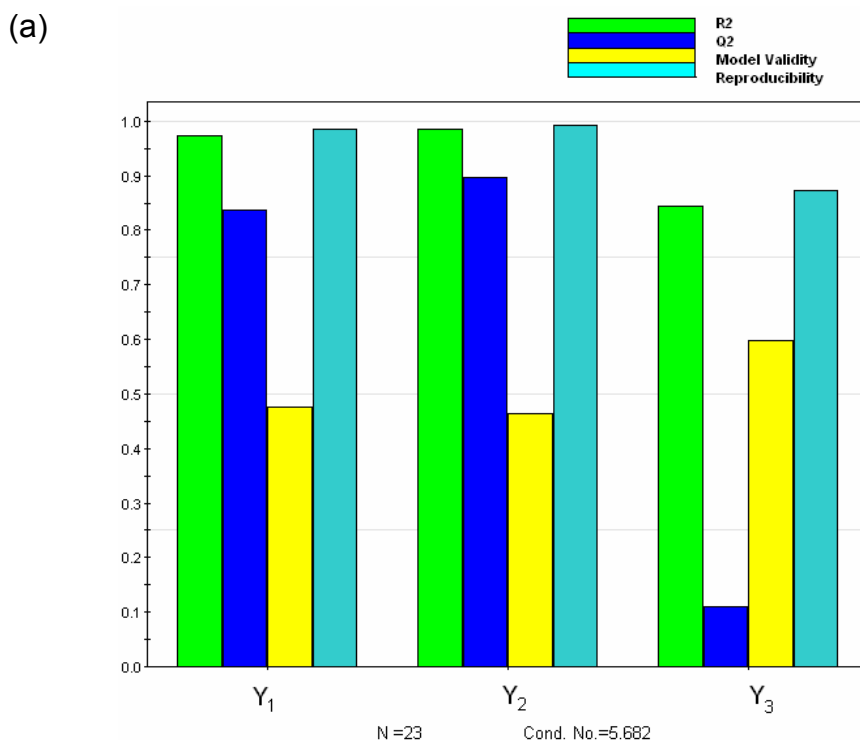
In general, SEM observations indicate that the higher the polymer solution concentration and clay loading, the more uniform, bead free and fibrous the structure tends to be.

### **Regression analysis**

Multiple linear regression analysis (MLR) was carried out to evaluate the contribution of the three factors to the morphology of the nanocomposite collected mats and to recognize the proper experimental settings space for optimizing their fibrous structure. It was found that the three measured responses ( $y_1 \equiv D_{\text{fibre}}$ ,  $y_2 \equiv N_{\text{bead}}$ ,  $y_3 \equiv D_{\text{bead}}/D_{\text{fibre}}$ ) were not normally distributed and were skewed with a tail to the right. They were, therefore, transformed appropriately so that MLR could be conducted. The MLR analysis resulted in three quadratic model equations, one for each of the three responses.

Fig. 2 shows some results from the statistical analysis which refer to the goodness of fit ( $R^2$ ) and of prediction ( $Q^2$ ) of the quadratic equations for the transformed responses and to their validity and reproducibility, after the model has been refined for the insignificant terms present due to the 4-level qualitative factor of flow rate.

The  $Q^2$  value of the refined model for  $Y_3$  is small ( $<0.5$ ) and the difference between  $R^2$  and  $Q^2$  is well far from the region 0.2 - 0.3. This suggest that the refined model for  $Y_3$  cannot be trusted [12], although its model validity value ( $=0.5973$ ) and its reproducibility ( $=0.8721$ ) could be accepted. Thus, only the  $Y_1$  and  $Y_2$  model equations are taken into account in what follows.



(b)

Response	$R^2$	$Q^2$	Model Validity	Reproducibility
$Y_1$	0.9730	0.8361	0.4762	0.9846
$Y_2$	0.9845	0.8970	0.4639	0.9915
$Y_3$	0.8443	0.1111	0.5973	0.8721

**Fig. 2.** Model check for each of the three transformed responses based on results from regression analysis after model refinement: (a) graphical representation, (b) summarized on a table.

Based on these results, the important factors in the electrospinning of the polymer nanocomposite can be recognized and optimal conditions can be obtained for predetermined fiber diameters and morphologies of the electrospun mats.

### **Important factors**

In order to find the extent of the impact of the three factors to these responses, the plots of coefficients were obtained where the importance of the inputs (coefficients) can be ranked and presented in a bar chart as shown in Fig. 3. Since  $Y_1$  and  $Y_2$  have different ranges, the coefficients are normalized by dividing them with the standard deviation of their respective response. In absolute values, the higher the bar of a term, the more important the term is.

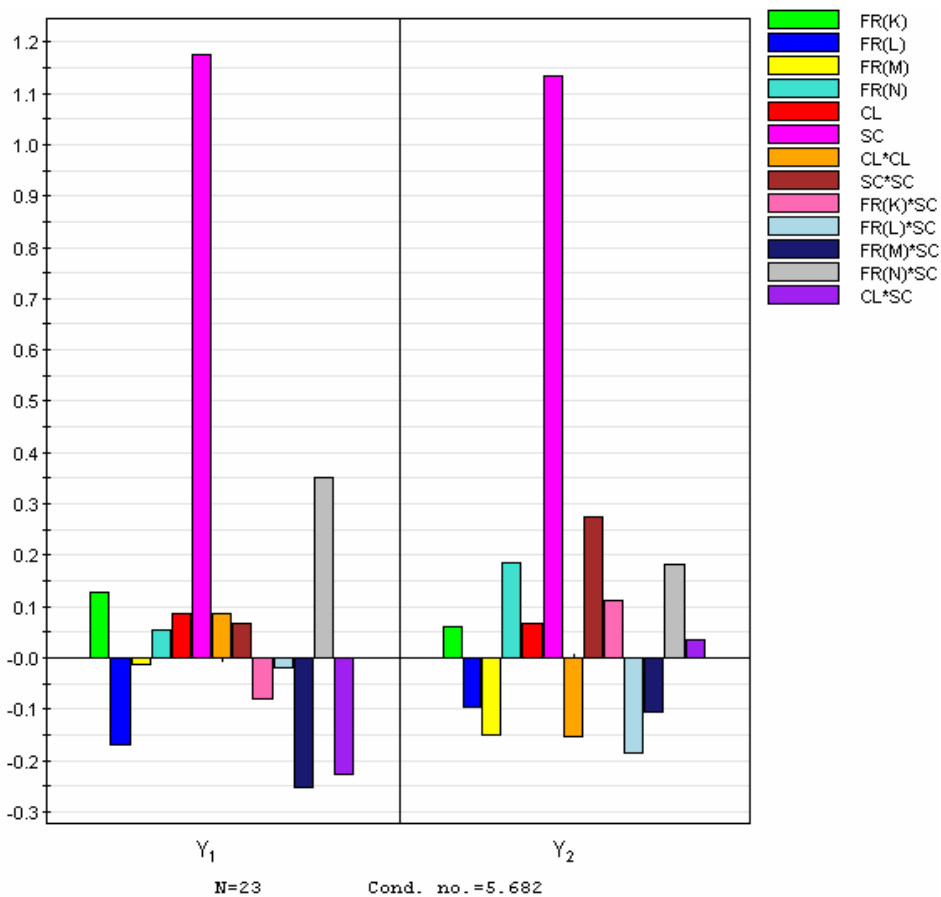


**Fig. 3.** The normalized coefficients plots for responses  $Y_1$  and  $Y_2$ .

The most striking feature of the obtained plots (Fig.3) is that for both responses  $Y_1$ (=transformed  $D_{\text{fiber}}$ ) and  $Y_2$ (=transformed  $N_{\text{bead}}$ ), polymer solution concentration (SC) is the eminent parameter. This great impact of SC on the responses overshadows the effect of the other terms and possibly if SC values were chosen within a different and less wide range, then other trends might be revealed.

### **Response surface results**

The contour plots for the two non-transformed responses  $D_{\text{fiber}}$  and  $N_{\text{bead}}$  were calculated with the aid of the corresponding model equations and were found similar for all four discrete levels of FR. The similarity of results for the four values of flow rate, which correspond to a tenfold increase in the flow rate, do suggest that this factor (FR) does not play any role on the fiber diameters and on the number surface density of beads. At Fig.4 the response surfaces for two flow rates are given.

For FR at the K-level (=0.5 ml/h), fibers at the 150 nm-scale of diameter are formed, when SC is low. Furthermore, when SC is low and below 7.5% w/v, the bead number density is high. Therefore, a mat is produced with fibers in the 150 nm-scale and with plenty of beads. On the other hand, the clay content in nanocomposite has only a minor effect on the diameter of the produced fibers ( $D_{\text{fiber}}$ ), since the contours are almost parallel to each other and almost parallel to the horizontal axis, which is the clay content axis (the plot consists of almost horizontal strips of different colour that represents a different fiber diameter value). The contour plot for the beads number density ( $N_{\text{bead}}$ ) is similar. It also consists of almost horizontal different-colour strips and therefore, the clay content has a minor effect on the number of the produced beads, as well. In general, all contour plots

conjointly show that fiber diameters and number of beads per  $\mu\text{m}^2$  are affected by the polymer solution concentration in opposite ways: increase of SC results in increase in  $D_{\text{fiber}}$  and decrease in  $N_{\text{bead}}$ . If fibers at the 500 nm-scale are desired, the SC has to be high, over 10% w/v and even higher. At these values of SC, a very small number of beads will be formed in accordance with the experimental findings.

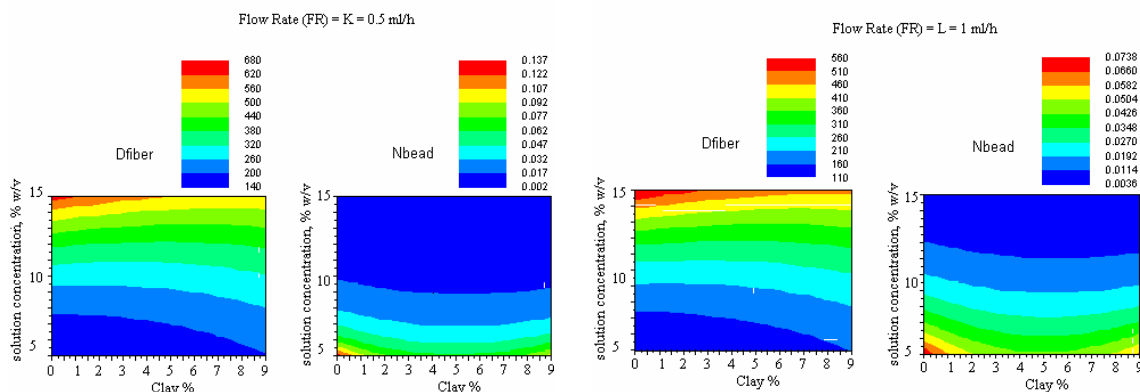


**Fig. 4.** The contour plots for the two non-transformed responses  $D_{\text{fiber}}$  and  $N_{\text{bead}}$  as a function of SC and CL at the 4 levels of FR.

For FR at the L-level (=1.0 ml/h), the same picture evolves. In this case, however, the window of very low bead number density is narrower than that for FR at the K-level. This only suggests that an even higher than 12% w/v solution concentration is necessary, if we are to produce fibers with just a few beads and diameters in the 500 nm-scale.

All the above response surface results are in good agreement with the experimental findings and show the way for further experimentation. The polymer solution concentration ought to be set in a more extended region; higher concentrations than the ones used here should be employed.

## Conclusions

A statistically sound quadratic model was built for the fiber diameter and the bead number density of the electrospun non-woven mats of a biodegradable-polymer nanocomposite following the DoE methodology and using a 25-run D-optimal design. The conclusions of the present study can be stated as it follows:

1. The model showed and the experimental findings ensured that the most crucial factor for the morphology of the electrospun mats is polymer solution concentration.
2. The clay content in the nanocomposite has a minor effect on the fiber diameters and the bead number density, when compared to the effect of the solution concentration at the processing conditions chosen, while the flow rate does not play any role, despite its wide value range.
3. Fiber diameters and number of beads per  $\mu\text{m}^2$  are affected by the polymer solution concentration in opposite ways.
4. Further experiments with a broader range in the experimental settings (particularly in solution concentration) should be designed incorporating even more factors such as the applied voltage and/or the room relative humidity in order to improve the process.
5. Optimization of the mat's morphology can be achieved by putting specific goals regarding the desired mat morphology and by choosing the experimental settings domain with the help of the results presented here.

## References

1. Berkland C, Pack DW, and Kim K. *Biomaterials* 2004;25(25):5649-5658.
2. Huang ZM, Zhang YZ, Kotaki M, and Ramakrishna S. *Composites Science and Technology* 2003;63(15):2223-2253.
3. Ji Y, Li BQ, Ge SR, Sokolov JC, and Rafailovich MH. *Langmuir* 2006;22(3):1321-1328.
4. Fong H, Liu WD, Wang CS, and Vaia RA. *Polymer* 2002;43(3):775-780.
5. Ristolainen N, Heikkila P, Harlin A, and Seppala J. *Macromolecular Materials and Engineering* 2006;291(2):114-122.
6. Daga VK, Helgeson ME, and Wagner NJ. *Journal of Polymer Science Part B-Polymer Physics* 2006;44(11):1608-1617.
7. Wang A, Hsieh AJ, and Rutledge GC. *Polymer* 2005;46(10):3407-3418.
8. Lee YH, Lee JH, An IG, Kim C, Lee DS, Lee YK, and Nam JD. *Biomaterials* 2005;26(16):3165-3172.
9. Marras SI, Kladi KP, Tsvintzelis L, Zuburtikudis I, and Panayiotou C. *Acta Biomaterialia* 2008;4(3):756-765.
10. Marras SI, Tsimliaraki A, Zuburtikudis I, and Panayiotou C. *Journal of Physics: Conference Series* 2007; 61, 1366-1370.
11. Marras SI, Tsimliaraki A, Zuburtikudis I, and Panayiotou C. *Polymer Engineering and Science*, in press.
12. Eriksson L, Johansson E, Kettaneh-Wold N, Wikstrom C, and Wold S. *Design of Experiments – Principles and Applications*, ISBN 91-973730-0-1, 2000.